

Neuron, Volume 111

Supplemental information

**Local 5-HT signaling bi-directionally
regulates the coincidence time window
for associative learning**

Jianzhi Zeng, Xuelin Li, Renzimo Zhang, Mingyue Lv, Yipan Wang, Ke Tan, Xiju Xia, Jinxia Wan, Miao Jing, Xiuning Zhang, Yu Li, Yang Yang, Liang Wang, Jun Chu, Yan Li, and Yulong Li

Figure S1

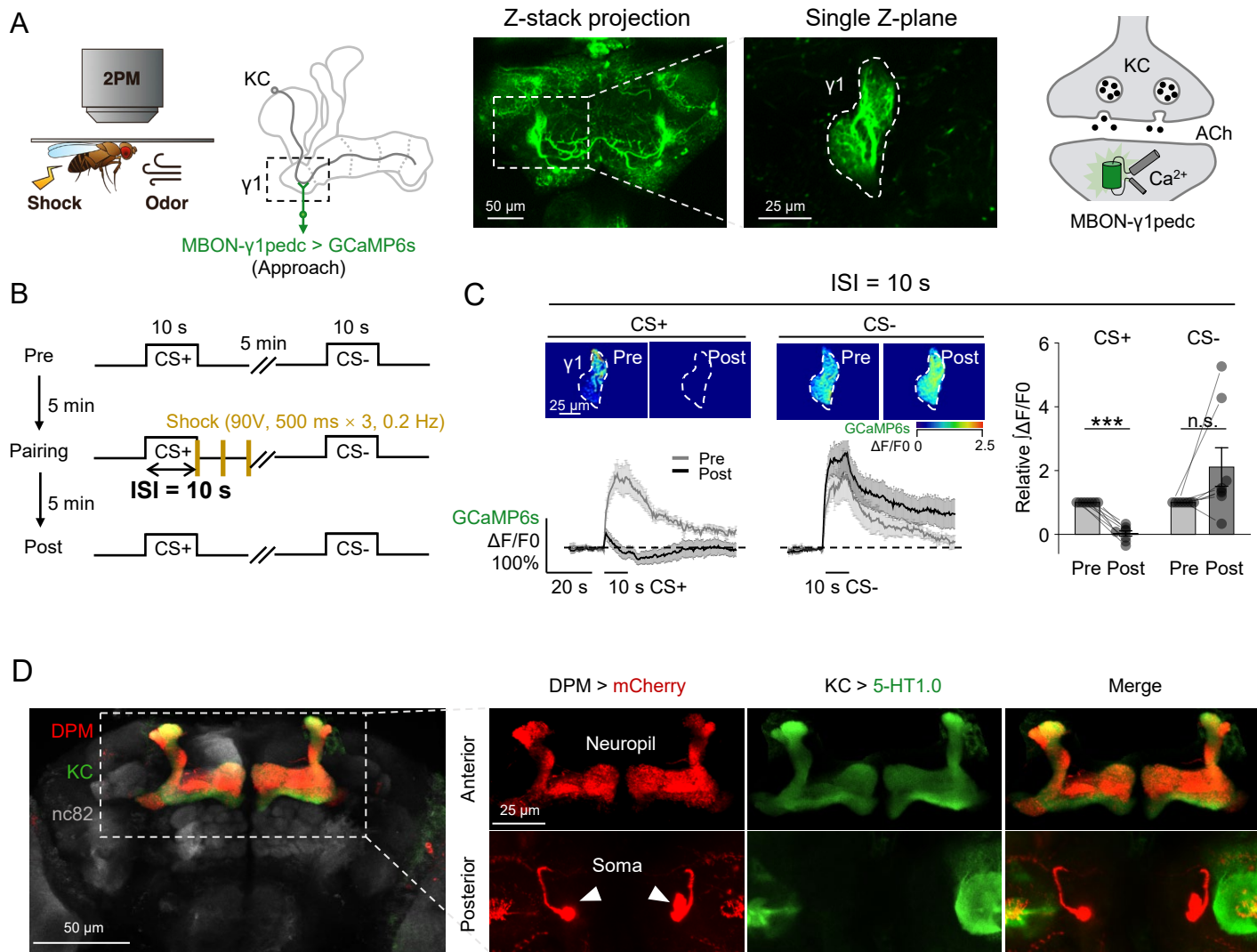


Figure S1. Ca²⁺ imaging in MBON-γ1pedc and the anatomy of the DPM neuron, related to Figures 2 and 3.

(A-C) The Ca²⁺ signal within MBON-γ1pedc reveals synaptic depression after odor-shock pairing. Schematics depicting the *in vivo* two-photon imaging setup, representative fluorescence images **(A)**, and the experimental protocol **(B)** for measuring changes of the Ca²⁺ signal with GCaMP6s expressed in the MBON-γ1pedc. Representative pseudo-color images **(C, top left)**, average (\pm SEM) traces **(C, bottom left)** and group analysis **(C, right)** of the fluorescence signals of GCaMP6s in the pre- and post-pairing sessions; n=8 flies/group.

(D) Immunofluorescent images (Z-stack projection) of a dissected brain from the fly expressing CsChrimson-mCherry (red) in the DPM neuron and 5-HT1.0 (green) in the KCs. The brain was counterstained with the anti-nc82 (gray). The somata of two DPM neurons in the posterior side and the neuropil in the anterior side were indicated.

*** $p < 0.001$; and n.s., not significant (paired Student's *t*-test).

Figure S2



Figure S2. Changes in synaptic plasticity of ACh release from different γ lobe compartments of control flies, and flies with various genetic or pharmacological manipulations, related to Figures 2, 5 and 6.

Shown are average (\pm SEM) traces of the odor-evoked change in ACh3.0 fluorescence measured in pre- and post-pairing sessions with the indicated ISI.

Figure S3

Upstream cell -> DPM

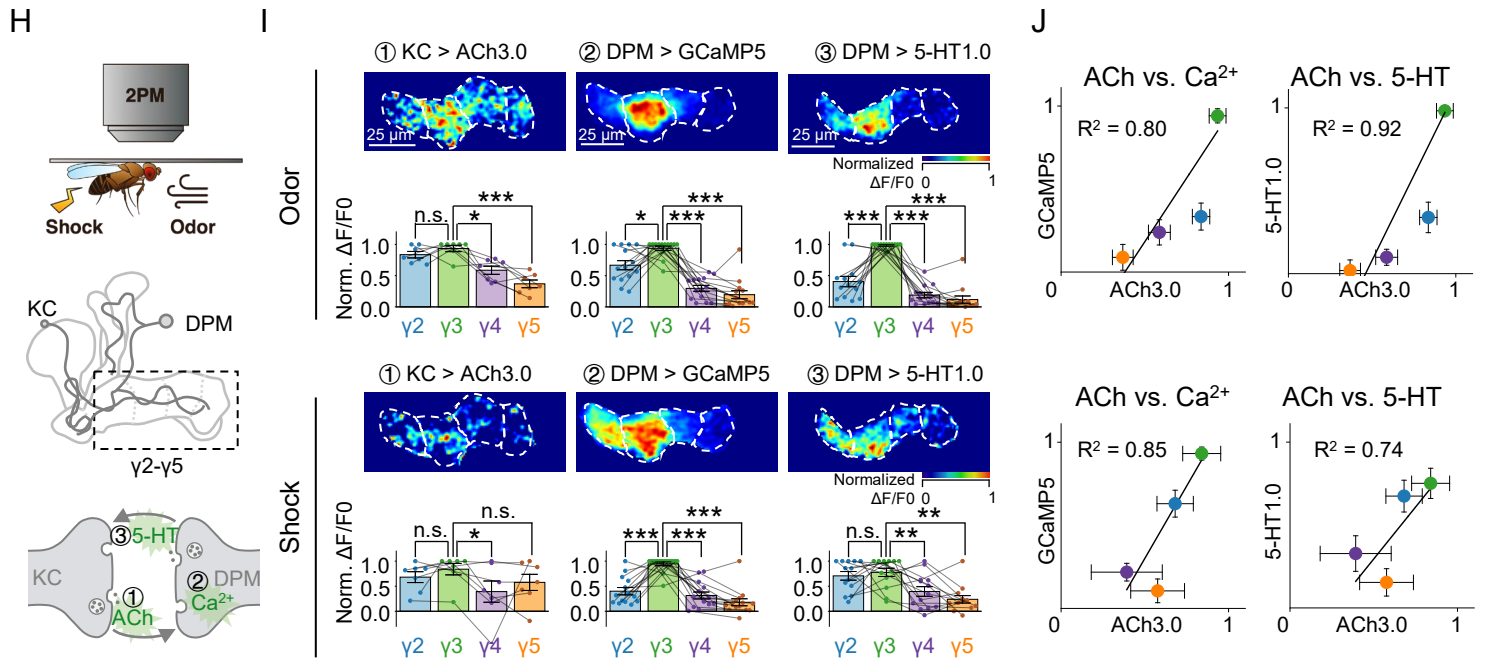
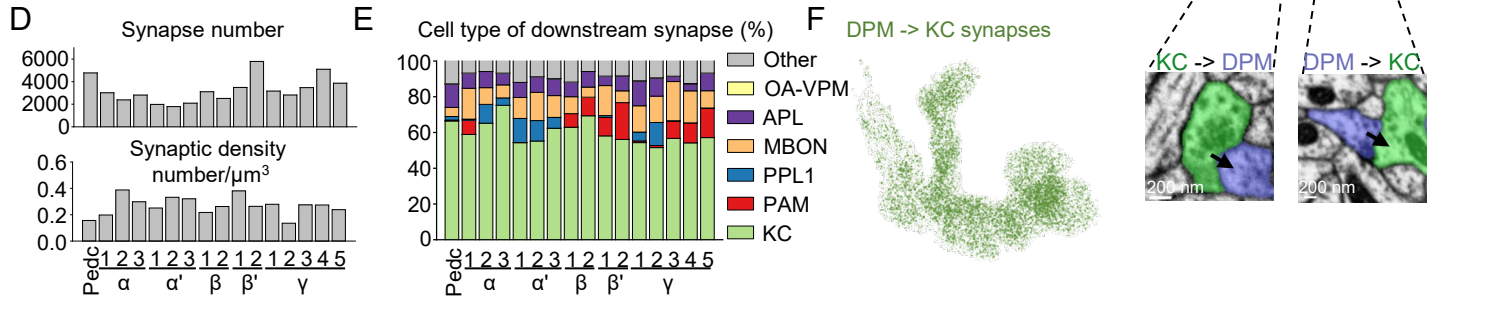
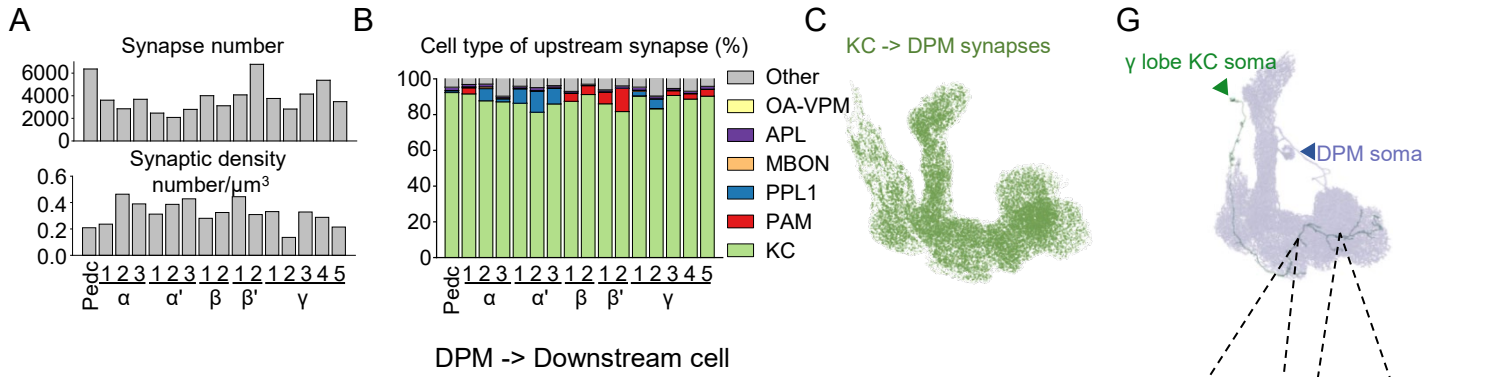


Figure S3. The DPM neuron and KCs are reciprocally connected and functionally correlated, related to Figures 3, 4 and 7.

(**A-G**) Analyzing MB EM connectomics reveals reciprocal connections between the DPM neuron and KCs. Shown are summary of the number of synapses (**A** and **D, top**), synaptic density (**A** and **D, bottom**), the percentage of synapses from indicated cell types (**B** and **E**), and the reconstruction of synapses from KCs (**C** and **F**) that are upstream or downstream of the DPM neuron in MB compartments. Also shown are reconstruction (**G, top**) and representative EM images (**G, bottom**) of a KC (green) forming reciprocal connections with the DPM neuron (blue) in the γ lobe. The arrows in the EM images indicate the direction from the presynapse to the postsynapse. The arrow heads in the reconstruction indicate the somata. Pedc, peduncle; OA-VPM, octopaminergic ventral paired median neuron; APL, anterior paired lateral neuron; MBON, mushroom body output neuron; PPL1, paired posterior lateral 1 cluster neuron; PAM, protocerebral anterior medial cluster neuron; KC, Kenyon cell. Version 1.1 of the hemibrain connectome [S1] was used for the analysis, and synapses with a confidence value >0.75 were included.

(**H-J**) The heterogenous patterns of 5-HT and Ca^{2+} dynamics of the DPM neuron are directly correlated with ACh release from KCs. Schematics (**H**), normalized pseudocolor images and summary (**I**) of ACh, Ca^{2+} and 5-HT signals in response to odor (1 s) or electric shock (0.5 s, 90 V) in the γ_2 - γ_5 compartments; $n=7$ -14 flies/group. For each fly, the fluorescence signals were normalized to the compartment with the highest response. Correlation analyses were performed by plotting the changes in Ca^{2+} or 5-HT dynamics (y -axis) against the changes in ACh release (x -axis) (**J**). The data were fitted to a linear function, and the R^2 is shown.

(**K-M**) Transcriptomic analysis of the DPM neuron, KCs of the γ lobe, and the APL neuron. The mAChRs and nAChRs in the DPM neuron (**K**; each point contains 123-130 cells). The 5-HT receptors in KCs of the γ lobe (**L**; each point contains ~ 2500 cells). The genetic markers for serotonergic and GABAergic neuron in the DPM neuron and the APL neuron (**M**; each point contains 123-130 DPM neurons or 20-36 APL neurons). Trhn, tryptophan hydroxylase neuronal; Ddc, DOPA-decarboxylase; Vmat, vesicular monoamine transporter; Gad1, glutamic acid decarboxylase 1; VGAT, vesicular GABA transporter. The published transcript database [S2] was used for analysis.

* $p < 0.05$; ** $p < 0.01$; *** $p < 0.001$; and n.s., not significant (paired Student's t -test).

Figure S4

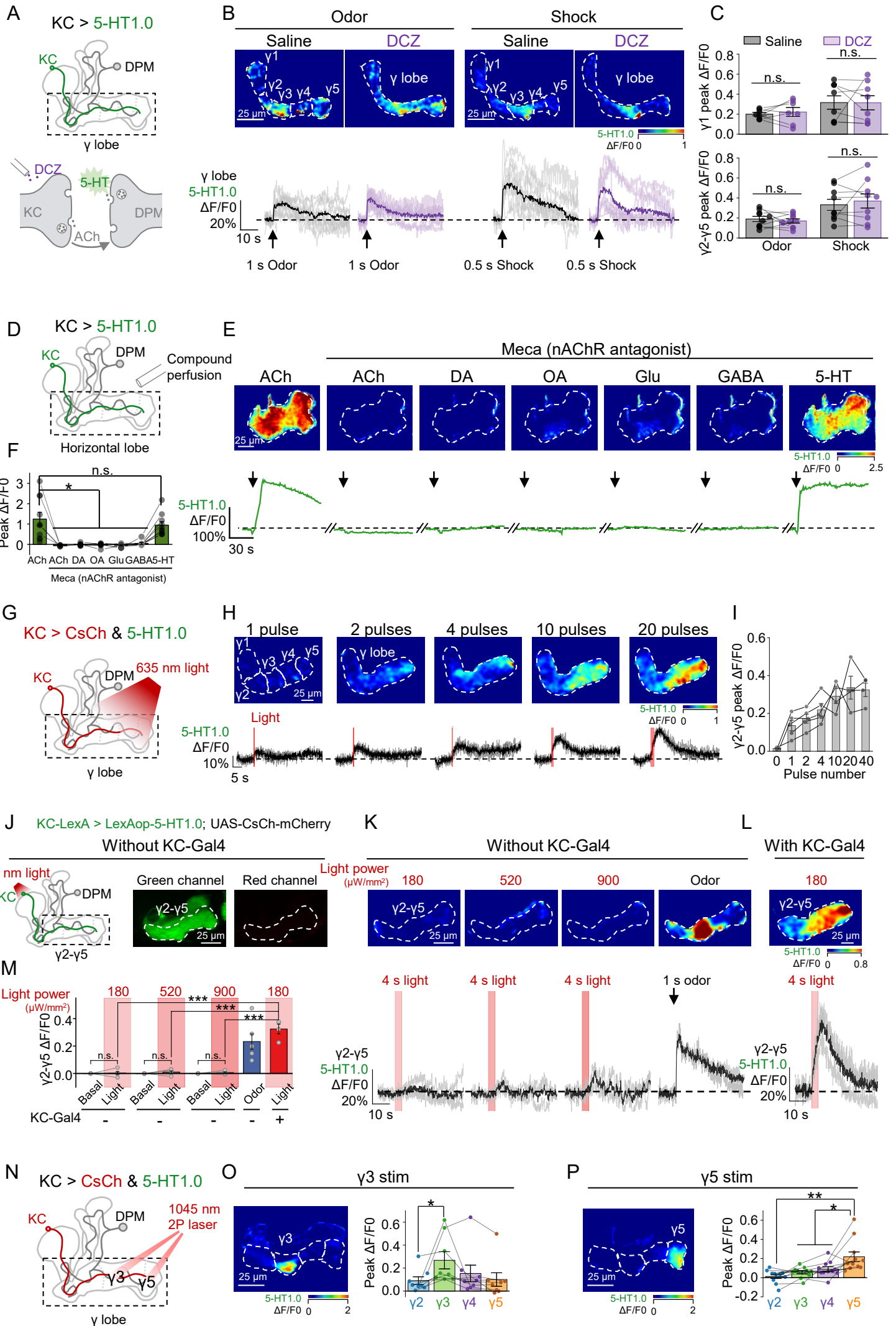


Figure S4. KCs release ACh to trigger 5-HT release from the DPM neuron, related to Figure 4.

(A-C) The hM4Di agonist DCZ does not cause significant effect on odor or shock-evoked 5-HT signals in the γ lobe. Shown are schematics depicting the *in vivo* imaging setup in which 5-HT was measured in the γ lobe using 5-HT1.0 expressed in KCs in the absence or presence of 30 nM DCZ (**A**). Also shown are representative pseudocolor images (**B, top**), average and individual traces (**B, bottom**), and group analysis of the change in 5-HT1.0 fluorescence from the γ 1 compartment (**C, top**) and γ 2- γ 5 compartments (**C, bottom**); n=7-9 flies/group. In each fly, the experiment was divided into saline and DCZ sessions, and in each session the odor and/or shock stimuli were applied for 1-3 trials, in random order.

(D-F) ACh application induces the release of 5-HT via nAChRs. Shown are schematics depicting the *in vivo* imaging setup in which 5-HT was measured in the γ lobe using 5-HT1.0 expressed in KCs (**D**). Also shown are representative pseudocolor images (**E, top**), single-trial traces (**E, bottom**), and summary of the change in 5-HT1.0 fluorescence from the MB horizontal lobe that includes the γ lobe (**F**) in response to application of the indicated neurotransmitters (1 mM) in the absence or presence of the nAChR antagonist Meca (100 μ M). ACh, acetylcholine; DA, dopamine; OA, octopamine; Glu, glutamate; GABA, gamma-aminobutyric acid.

(G-I) Optogenetically activating KCs induces a pulse number-dependent release of 5-HT in the γ lobe. Shown are schematics (**G**) depicting the *in vivo* imaging setup in which CsChrimson-expressing KCs were activated by light pulses (1 ms/pulse, 635 nm, 10 Hz), and 5-HT was measured in the γ lobe using 5-HT1.0 expressed in KCs. Also shown are representative pseudocolor images (**H, top**), average and individual traces (**H, bottom**), and summary of the change in 5-HT1.0 fluorescence in response to the indicated number of light pulses; n=4 flies. For each fly, experiments were divided into 3 sessions, and in each session 1, 2, 4, 10 and 20 pulses were delivered randomly.

(J-M) Light stimulation does not affect 5-HT dynamics in flies with UAS-CsChrimson but without KC-Gal4 driver, ruling out the unspecific effect caused by leaky expression of channelrhodopsin. Shown are schematics (**J, left**) and fluorescence images (**J, right**) depicting the *in vivo* imaging setup in which 5-HT was measured with 5-HT1.0 expressed in KCs, while the light pulses (1 ms/pulse, 635 nm, 10 Hz) were delivered to the brain of the fly only carrying UAS-CsCh-mCherry, but not KC-Gal4. Also shown are representative pseudocolor images (**K, L, top**), average and individual traces (**K, L, bottom**), and group analysis (**M**) of the change in 5-HT1.0 fluorescence in response to light pulses (4 s) with the indicated power or odor stimuli (1 s), in flies without or with KC-Gal4. Note that the data of flies with KC-Gal4 are reproduced from the saline group of Figures 4E-4F. Also note that light pulses with the power of 180 μ W/mm² were used in Figure 4D-4F and S4G-S4I.

(N-P) Optogenetically activating KCs in a spatially restricted manner induces local release of 5-HT. Shown are schematics (**N**) depicting the *in vivo* imaging setup in which a two-photon laser (1045-nm, 100-ms duration) was used to locally activate CsChrimson-expressing KCs and the 5-HT was measured in 5-HT1.0-expressing KCs. Also shown are representative pseudocolor images (**O and P, left**) and group analysis (**O and P, right**) of the change in 5-HT1.0 fluorescence in response to localized optogenetic stimulation in the γ 3 or γ 5 compartment; n=8-11 flies/group.

* p <0.05; ** p <0.01; *** p <0.001; and n.s., not significant (paired or unpaired Student's *t*-test).

Figure S5

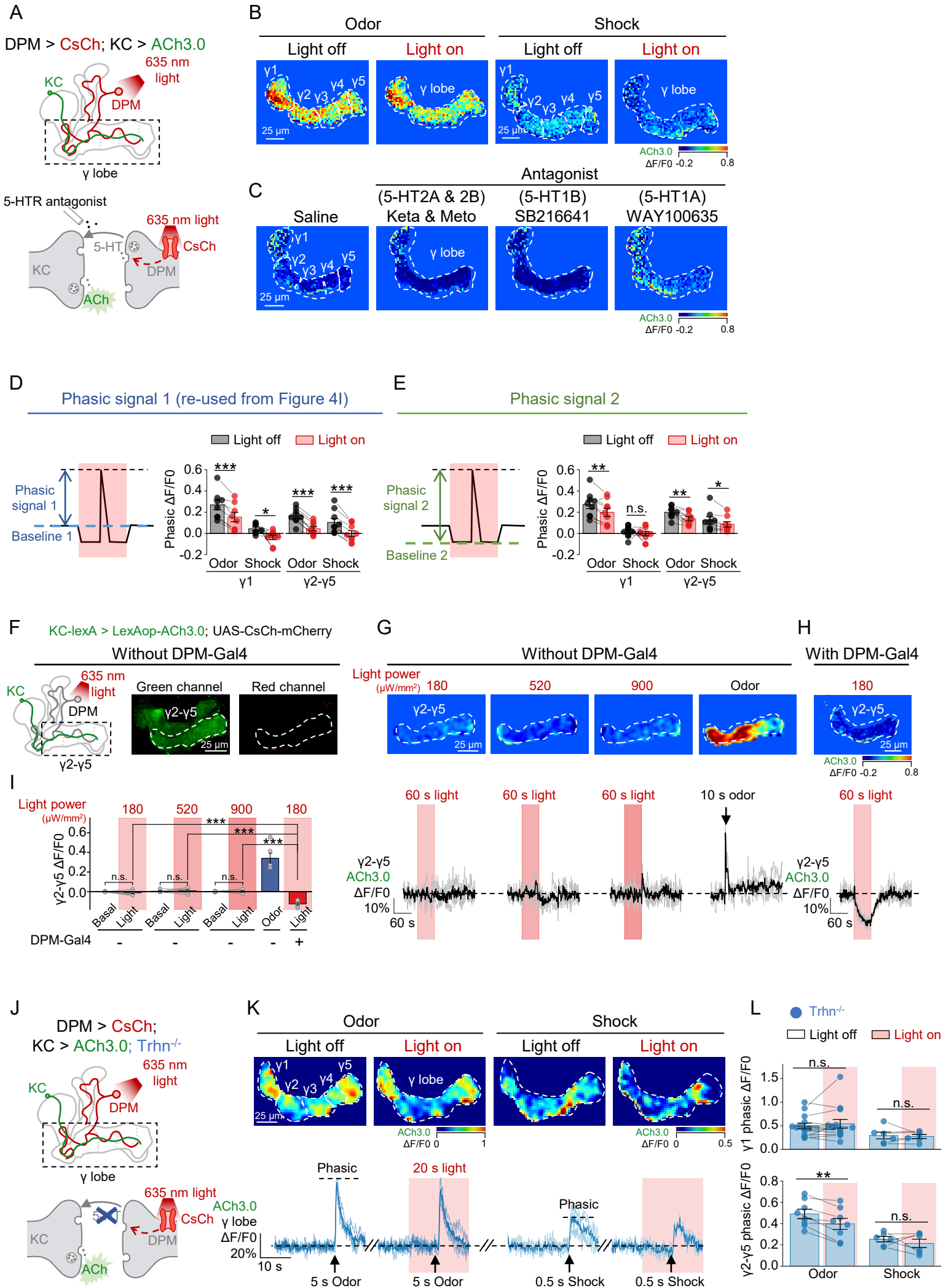


Figure S5. Optogenetically activating the DPM neuron inhibits both phasic and tonic release of ACh from KCs, related to Figure 4.

(A) Schematics depicting the *in vivo* imaging setup in which the CsChrimson-expressing DPM neuron was activated by light pulses (1 ms/pulse, 635 nm, 10 Hz), and ACh was measured in the γ lobe using ACh3.0 expressed in KCs.

(B-C) Representative pseudocolor images of the change in ACh3.0 fluorescence in response to odor (5-s application) or electric shock (0.5 s, 90 V) in the absence or presence of light stimulation **(B)**, or to 60-s light stimulation in the absence or presence of 5-HT receptors' antagonists **(C)**.

(D-E) Left: schematics depicting strategies for calculating the phasic ACh3.0 signals with different baselines. **Right:** summary of the phasic ACh3.0 signals measured in response to odor (1 s) or electric shock (0.5 s, 90 V) applied in the absence or presence of light stimulation; n=8-9 flies/group. Note that the summary data in **(D)** are reproduced from Figure 4I.

(F-I) Light stimulation does not affect ACh dynamics in flies with UAS-CsChrimson but without DPM-Gal4 driver, ruling out the unspecific effect caused by leaky expression of channelrhodopsin. Shown are schematics **(F, left)** and fluorescence images **(F, right)** depicting the *in vivo* imaging setup in which ACh was measured with ACh3.0 expressed in KCs, while the light pulses (5 ms/pulse, 635 nm, 10 Hz) were delivered to the brain of the fly only carrying UAS-CsCh-mCherry, but not DPM-Gal4. Also shown are representative pseudocolor images **(G, H, top)**, average and individual traces **(G, H, bottom)**, and group analysis **(I)** of the change in ACh3.0 fluorescence in response to light (60 s) with the indicated power or odor stimuli (10 s), in flies without or with DPM-Gal4. Note that the data of flies with DPM-Gal4 are reproduced from the saline group of Figures 4J-4K and S5C. Also note that light pulses with the power of 180 $\mu\text{W}/\text{mm}^2$ were used in Figures 4J-4K and S5C. The gap junction blocker CBX (100 μM) was present throughout the experiment.

(J-L) Optogenetically activating the DPM neuron-elicited decrease of the phasic ACh signal is diminished in *Trhn^{-/-}* flies. Shown are schematics **(J)** depicting the *in vivo* imaging setup in which the CsChrimson-expressing DPM neuron was activated by light pulses (5 ms/pulse, 635 nm, 10 Hz), and ACh was measured in the γ lobe using ACh3.0 expressed in KCs of *Trhn^{-/-}* flies. Also shown are representative pseudocolor images **(K, top)**, average and individual traces **(K, bottom)**, and group analysis **(L)** of the change in ACh3.0 fluorescence in response to odor (1 s) or electric shock (0.5 s, 90 V) in the absence or presence of light; n=6-12 flies/group. A fly received 2-8 pairs of odor and/or shock stimuli, and within each pair the light-on and light-off trials were performed in random order. Note that the gap junction blocker CBX (100 μM) was present throughout these experiments.

* $p < 0.05$; ** $p < 0.01$; *** $p < 0.001$; and n.s., not significant (paired or unpaired Student's t-test).

Figure S6

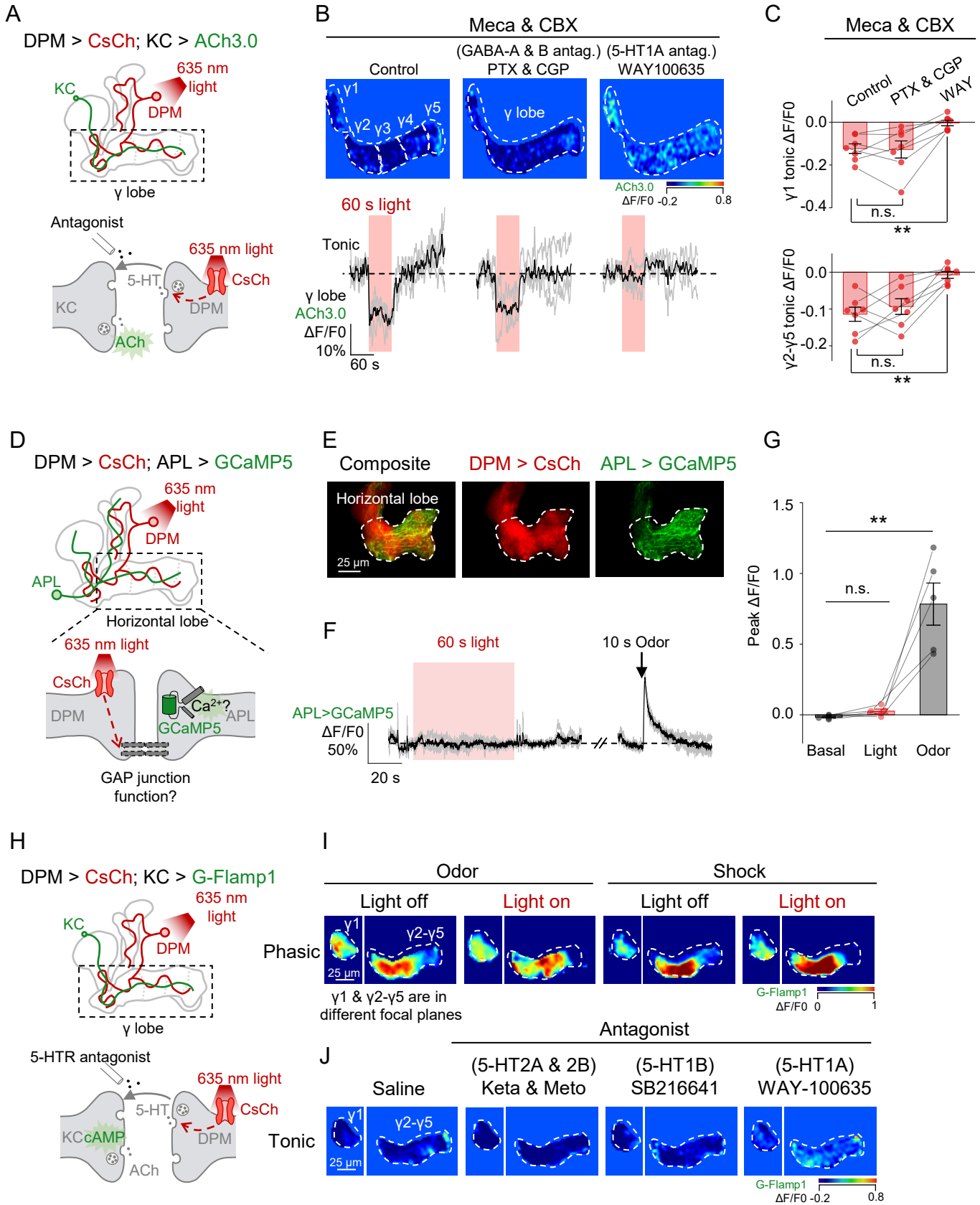


Figure S6. Optogenetically activating the DPM neuron inhibits ACh and cAMP signals of the KCs, but does not affect the Ca²⁺ signal of the APL neuron, related to Figure 4.

(A-C) DPM activation-induced inhibitory effect on the tonic ACh signal is mediated by 5-HT, instead of GABA. Shown are schematics **(A)** depicting the *in vivo* imaging setup in which the CsChrimson-expressing DPM neuron was activated by light pulses (5 ms/pulse, 635 nm, 4 Hz), and ACh was measured in the γ lobe using ACh3.0 expressed in KCs in the absence or presence of antagonists of GABA and 5-HT receptors. Also shown are representative pseudocolor images **(B, top)**, average and individual traces **(B, bottom)**, and summary **(C)** of the change in ACh3.0 fluorescence in response to a 60-s light pulse. Where indicated, the GABA-A receptor antagonist picrotoxin (PTX, 125 μ M), the GABA-B receptor antagonist CGP54626 (CGP, 25 μ M), and the 5-HT_{1A} receptor antagonist WAY-100635 (WAY, 20 μ M) were applied; n=7 flies/group. For each fly, the experiment was divided into 3 sessions, and each session contains 3 repetitive trials. Note that the nAChR antagonist Meca (30 μ M) and the gap junction blocker CBX (100 μ M) were present throughout the imaging experiments.

(D-G) Optogenetically activating the DPM neuron does not cause significant effect on the Ca²⁺ signal of the APL neuron. Shown are schematics **(D)** and representative fluorescence images **(E)** of the *in vivo* imaging setup, in which the CsChrimson-expressing DPM neuron was activated by light (1 ms/pulse, 635 nm, 10 Hz), and the Ca²⁺ signal was measured using GCaMP5 expressed in the APL neuron. Also shown are average and individual traces **(F)**, and summary **(G)** of the change in GCaMP5 fluorescence in response to light (60 s) or odor (10 s); n= 5 flies/group. Each fly received 3 trials of light stimulation and 3 trials of odor stimulation in random order.

(H-J) Activating the DPM neuron only inhibits tonic cAMP dynamics, but does not influence phasic cAMP increase evoked by odor or shock stimuli in the γ lobe. Shown are schematics **(H)** depicting the *in vivo* imaging setup in which the CsChrimson-expressing DPM neuron was activated by light pulses (5 ms/pulse, 635 nm, 4 Hz) and cAMP was measured in the γ lobe using G-Flamp1 expressed in KCs. Also shown are representative pseudocolor images of the change in G-Flamp1 fluorescence in response to odor (5-s application) or electric shock (0.5 s, 90 V) in the absence or presence of light stimulation **(I)**, or to 60-s light stimulation in the absence or presence of 5-HT receptors' antagonists applied at 20 μ M **(J)**.

** $p < 0.01$ and n.s., not significant (paired Student's *t*-test).

Figure S7

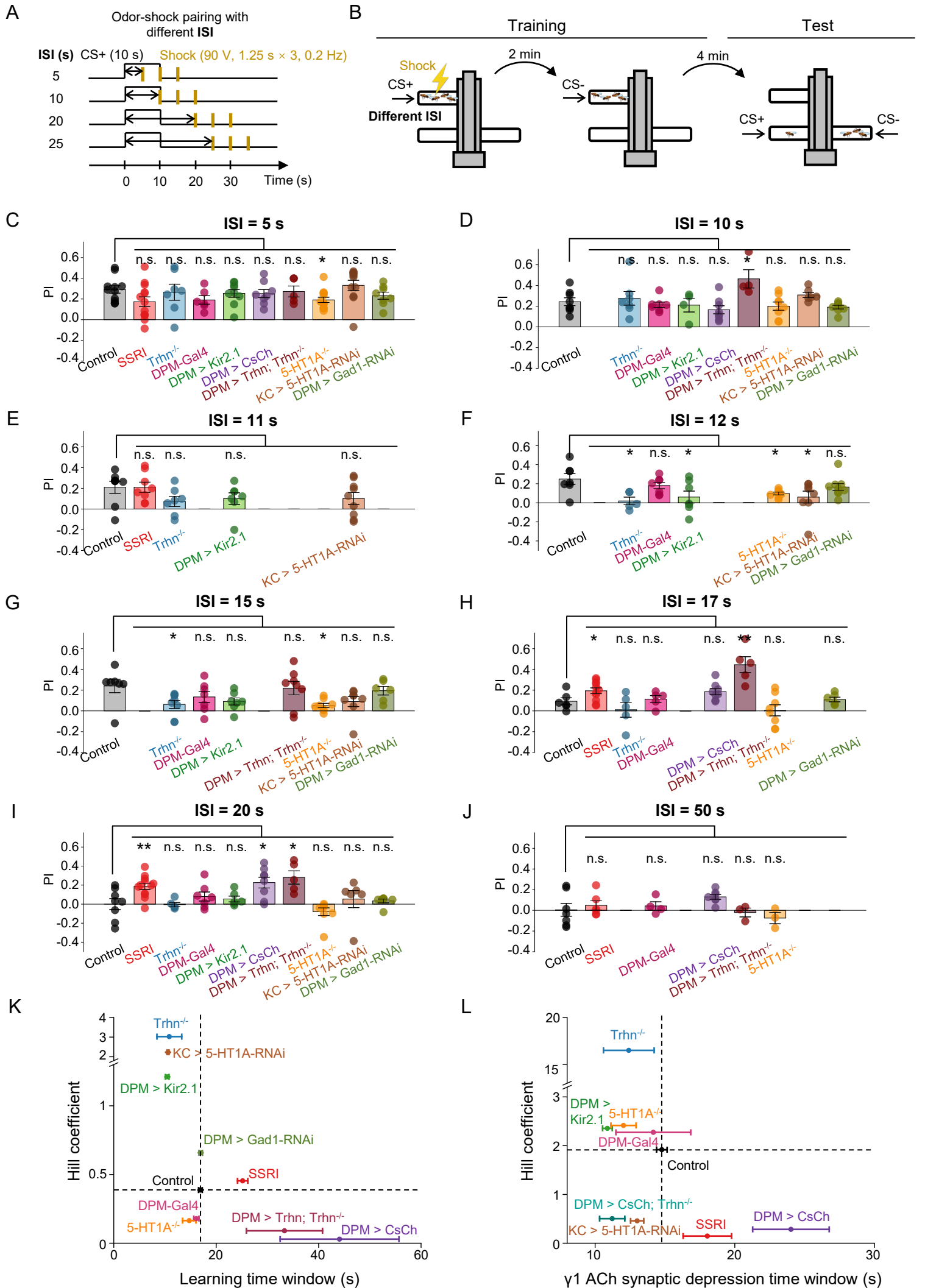


Figure S7. Summary of the PIs, Hill coefficients and coincidence time windows, related to Figure 8.

(A-B) Schematics depicting the protocol for odor-shock pairing with varying ISIs (A) and the T-maze assay for measuring the olfactory memory (B).

(C-J) Summary of the PIs measured using the indicated ISI of flies with various genetic or pharmacological manipulations; n=3-11 for each group.

(K-L) Correlation analysis between the Hill coefficient and the length of coincidence time window ($t_{50} \pm$ standard error) of flies with various genetic or pharmacological manipulations. The dashed lines indicate the values of control flies.

Note that the data in (C-K) are reproduced from Figures 1 and 7, and data in (L) are reproduced from Figures 2 and 5.

* $p < 0.05$; ** $p < 0.01$; and n.s., not significant (unpaired Student's *t*-test).

Figure S8

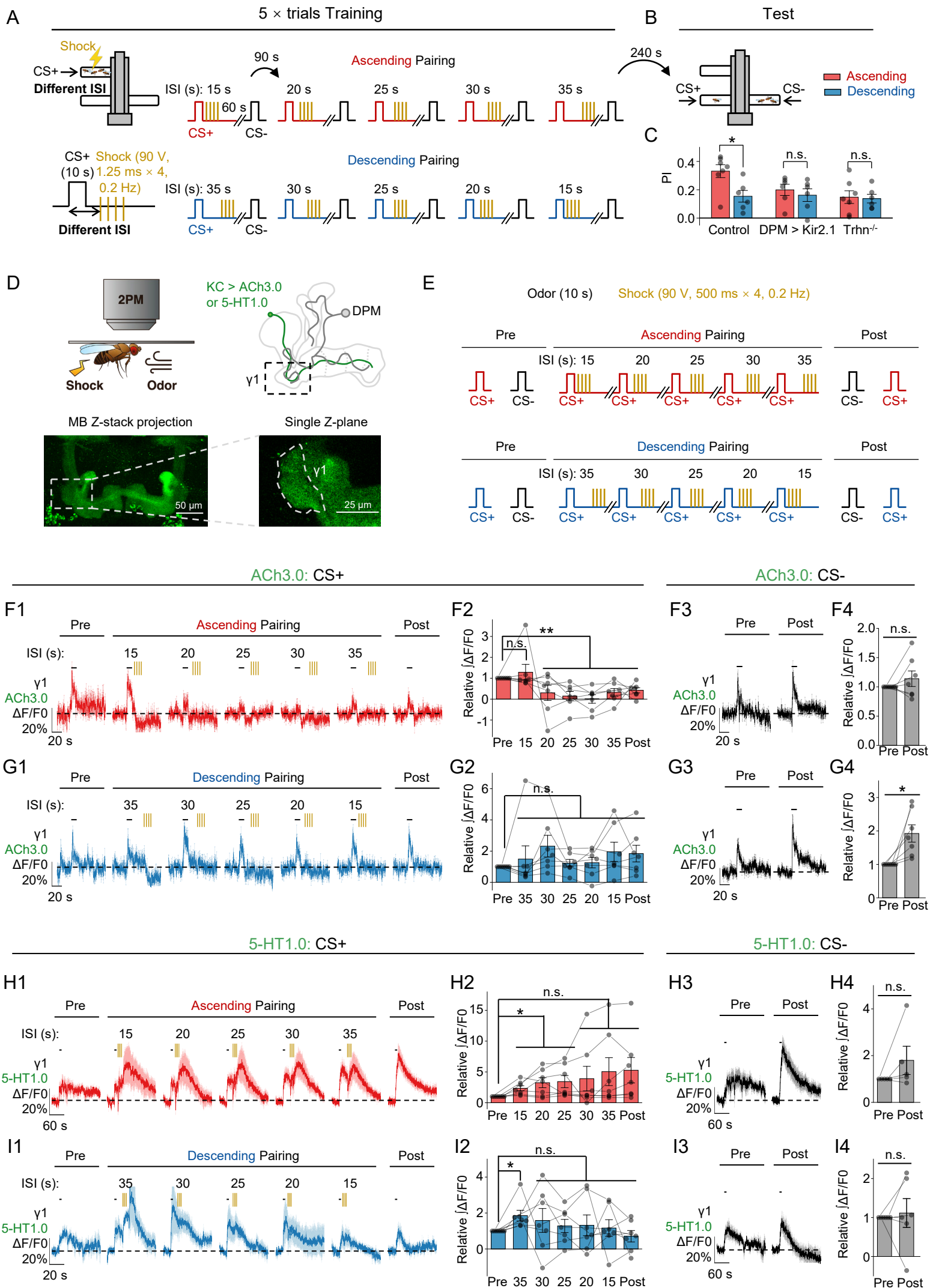


Figure S8. 5-HT from the DPM neuron helps to bridge the CS-US temporal gap, related to Figure 8.

(A-C) Schematics depicting different protocols for ascending and descending pairing paradigms (A-B) and summary of PIs (C) measured in control flies, DPM > Kir2.1 flies, and Trhn^{-/-} flies; n=6-7 for each group.

(D-E) Schematics depicting the *in vivo* two-photon imaging setup (D, top), fluorescence images (D, bottom), and the ascending and descending pairing protocols (E) for measuring the change in ACh or 5-HT dynamics in the MB γ 1 compartment with ACh3.0 or 5-HT1.0 expressed in KCs.

(F-G) Shown are average (\pm SEM) traces and summary of ACh release measured in the ascending (F) or descending (G) pairing paradigms in response to CS+ or CS-; n=6-7 flies/group.

(H-I) Similar to (F-G), except that 5-HT dynamics were measured and analyzed.

* $p < 0.05$; ** $p < 0.01$; and n.s., not significant (paired or unpaired Student's *t*-test).

SUPPLEMENTAL REFERENCES

1. Scheffer, L.K., Xu, C.S., Januszewski, M., Lu, Z., Takemura, S.Y., Hayworth, K.J., Huang, G.B., Shinomiya, K., Maitlin-Shepard, J., Berg, S., et al. (2020). A connectome and analysis of the adult *Drosophila* central brain. *Elife* 9. [10.7554/eLife.57443](https://doi.org/10.7554/eLife.57443).
2. Aso, Y., Ray, R.P., Long, X., Bushey, D., Cichewicz, K., Ngo, T.T., Sharp, B., Christoforou, C., Hu, A., Lemire, A.L., et al. (2019). Nitric oxide acts as a cotransmitter in a subset of dopaminergic neurons to diversify memory dynamics. *Elife* 8. [10.7554/eLife.49257](https://doi.org/10.7554/eLife.49257).